

Long-term SWRO Testing of Nanocomposite Membranes

CJ Kurth*, R. Burk*, J.Green*, J. LEPARC**, P. Choules***

*750 Lairport Street, El Segundo, CA 90245

**Anjou Recherche, Chemin de la Digue –BP76, 78603 Maisons-Laffitte cedex, France

***4760 World Houston Parkway, Suite 140, Houston, TX 77032

Abstract

Nanocomposite seawater reverse osmosis (SWRO) membranes were prepared and rolled into 4” spiral wound modules. These high-flux modules were tested using open intake seawater feed over the course of 1 year, including high flux operation during a red tide event. Over the test period the modules exhibited promising fouling resistance and high permeability characteristics, and were stable through repeated cleanings. Subsequent element autopsy was performed to determine the chemical and biological foulants present within the module. Results indicate the primary foulants were biological in nature with reduced levels of inorganics also present.

Keywords

SWRO; nanocomposite membrane; TFN; fouling; high flux; foulant analysis

INTRODUCTION

Permeability and fouling resistance are key economic drivers for membrane-based water treatment systems. These performance characteristics translate directly to the energy intensity and capital expenditures of a reverse osmosis (RO) system and therefore to the economics of desalination. Accounting for 70-80% of the total expense of RO desalinated water, energy consumption and capital expenditures are the primary reason why desalination remains expensive compared to most freshwater sources (USBR 2003).

Thin film nanocomposite (TFN) membranes were developed through the dispersion of zeolite nanoparticles in a traditional polyamide thin film (Jeong et al, 2007). Incorporation of such nanoparticles into a brackish water reverse osmosis (BWRO) membrane formulation increased permeability and altered surface properties potentially related to fouling, while maintaining salt rejection. These are the changes that applied to SWRO are needed to lower the cost of desalination. Since the original publication of the TFN concept, TFN membrane technology has been optimized for use in SWRO. Transmission Electron Microscope (TEM) imaging has demonstrated the incorporation of nanoparticles into a conventional polyamide thin-film membrane (Kurth et al, 2009). Membrane performance data, using industry-standard cross-flow testing, demonstrates a doubling of TFN membrane permeability relative to conventional RO membranes with equivalent rejection. For example, TFN technology transforms an industry standard 17 GFD (gallons per square foot per day) membrane into a 33 GFD membrane. Current performance of TFN membranes leads to elements possessing in an enhanced flux of more than double that of a 24.6m³/d (6,500 gpd) commercial baseline with salt rejection at industry standards.

METHODS

Flat-sheet Membrane Equipment

Testing of flat-sheet membranes was performed on stainless steel cells obtained from Delstar Technologies. Cells were used without a feed spacer (unless noted) and had an active area of 19.4 cm² (3 in²). Test benches, shown in Figure 1, were configured with 6 cells, (two parallel sets of 3 cells in series).



Figure 1: Flat-sheet Cell Testing Bench

Individual permeate flow meters were equipped to allow real time measurement of permeate flow rates with programmable logic controller (PLC) data logging. Each bench was equipped with a 5-gallon feed reservoir, a chiller to maintain temperature and a 1 micron polypropylene depth filter. Salinities were measured with a Hach Sension 5 Conductivity/TDS/Salinity meter calibrated at two concentrations daily.

Membrane Fabrication

Membranes were prepared by a process widely described in the literature (Jeong et al, 2007; Ghosh et al, 2008; Cadotte 1981). After preparation, membranes were refrigerated until testing. In all cases, hand-cast membranes were tested within four days of synthesis.

Short-term Testing Procedure

Membrane performance was typically measured after 1 hour of operation. For clean waters (NaCl in tap water with an in-line filter), this performance was found to accurately indicate longer-term performance. Feed temperature was maintained at 25° C to within 1° C; feed salinity was maintained at 32,000 ppm to within 500 ppm. After a 1 hour stabilization period at 800 psi, flux was determined by measuring permeate volume collected in a fixed time interval and salt passage measured by conductivity measurements on the feed and the obtained sample. Individual flux and rejection measurements were normalized for pressure and temperature to 25° C and 32,000 ppm based on known equations (Dow 2010).

Long-term Testing Procedure

For long-term tests (longer than 1 hour), performance was determined in a manner similar to that of the short-term tests with the following differences: feed water was changed to a mixed salt solution more closely matching that of seawater (Instant Ocean™) in DI water. No in-line filter was used allowing measurable turbidity to accumulate during the test [typically 1 Nephelometric Turbidity Unit (NTU)].

Element Field Testing Procedure

Feed water at the U.S. Navy Seawater Desalination Test Facility at Port Hueneme, California, USA (SDTF) facility enters through a screen-fed open ocean intake and passes to a facility wide intermediate tank. This tank feeds one of two pretreatment systems. For the first 4,700 hours of testing a single stage media filter was used, for the remainder of the test a Zenon ultrafiltration (UF) pretreatment system was used. The media filter contained anthracite, garnet, and fine and coarse gravel followed by a single stage 5 micron cartridge filter.

The pilot system pictured in Figure 2 consisted of five, two-element vessels plumbed in series. For all data contained here only three of the five vessels were employed resulting in a six-element in series, single-pass array configuration. Each end cap of the vessels was equipped with a permeate port. Because plugged interconnectors were used between each element, independent permeate flow and rejection was quantified for each element in the system. The permeate solutions were then sent to a common manifold and blended into a totalized permeate stream allowing system performance to be monitored.



Figure 2: Element test system at Port Hueneme

Data was typically collected manually once daily, although more frequent testing was often performed after element changes or cleanings. Feed water quality was measured between two to five times per week by a single water quality setup. The metrics monitored were raw water turbidity and RO feed turbidity, Silt Density Index (SDI) and particle count.

Element Cleaning Procedure

The elements were first recirculated with a solution of 2% ethylenediaminetetraacetic acid (EDTA) at pH 11.8 (with NaOH) in RO permeate at 75 psi and 28° C for one hour. This was then neutralized, drained, and the system was fed with a 1.4% solution of citric acid in water (pH 2.3). This solution was recirculated for 2 hours at 75 psi and 29.7° C. The system was then shut down and the elements were allowed to soak in this solution overnight. The following morning the solution was neutralized and drained. A third high pH clean was then used for the CIP at ~1000 hours. A 3% solution of General Electric (GE) RO membrane cleaner at a pH of 11.1 was recirculated for 2 hours at 87 psi and 30° C.

The second cleaning that was performed replaced the initial EDTA clean with the GE RO cleaning solution and was followed by the citric acid cleaning. No third cleaning step was performed for the second CIP.

Element Autopsy Procedure

Autopsy of the long-term element was conducted by staff at Veolia Water's Anjou Recherche facility. The autopsy was performed on the lead element. The long-term test element was removed from the packaging material and visually inspected. Once opened, the overall appearance was noted, and a brown residual deposit present on the membrane was removed and collected.



Figure 3: Brown Deposit

This deposit shown in Figure 3 was subjected to the following analyses:

- Scanning Electron Microscopy (SEM) for deposit morphology
- SEM/Energy Dispersive X-ray (EDX) for atomic composition
- Dry matter and loss on ignition
- Total Organic Content (TOC)
- Carbohydrate analysis by the Dubois method (Dubois et al, 1956)
- ATR-FTIR for chemical analysis
- Total cell quantification by 4',6-diamidino-2-phenylindole (DAPI) staining to evaluate the microbiological content

RESULTS AND DISCUSSION

TFN Membrane Performance

To determine the performance of TFN membranes relative to commercial products, longer-term flat-sheet tests were performed. These tests were performed with the TFN membranes and a competitive high flux seawater membrane (equivalent to that used in 9,000 gpd elements) in parallel (tested at the same time, pressure, cross-flow conditions and feed water). Over the first 20 hours both membranes lost flow because of the presence of turbidity on the bench (no prefiltration was used, turbidity ~1 NTU) led to fouling of both membranes (Figure 4). At 20 hours the membranes were cleaned with a pH 11 NaOH solution containing 50 ppm of EDTA for 30 minutes. After the bench cleaning, the flux of the TFN membrane recovered to its initial value, while relatively little of the commercial membrane's flux was restored. This difference in flux recovery after cleaning is ascribed to altered surface properties of the TFN membrane. The test was then resumed with a similar loss of flux over the next 20 hours after which performance was stable for the remainder of the test. After a rinse period, rejection of the TFN membrane was above 99.7% for the duration of the test.

Although initial flux of the competitive product met listed flux specification, fouling over the first 20 hours dropped flux to a reduced level that cleaning did not restore.

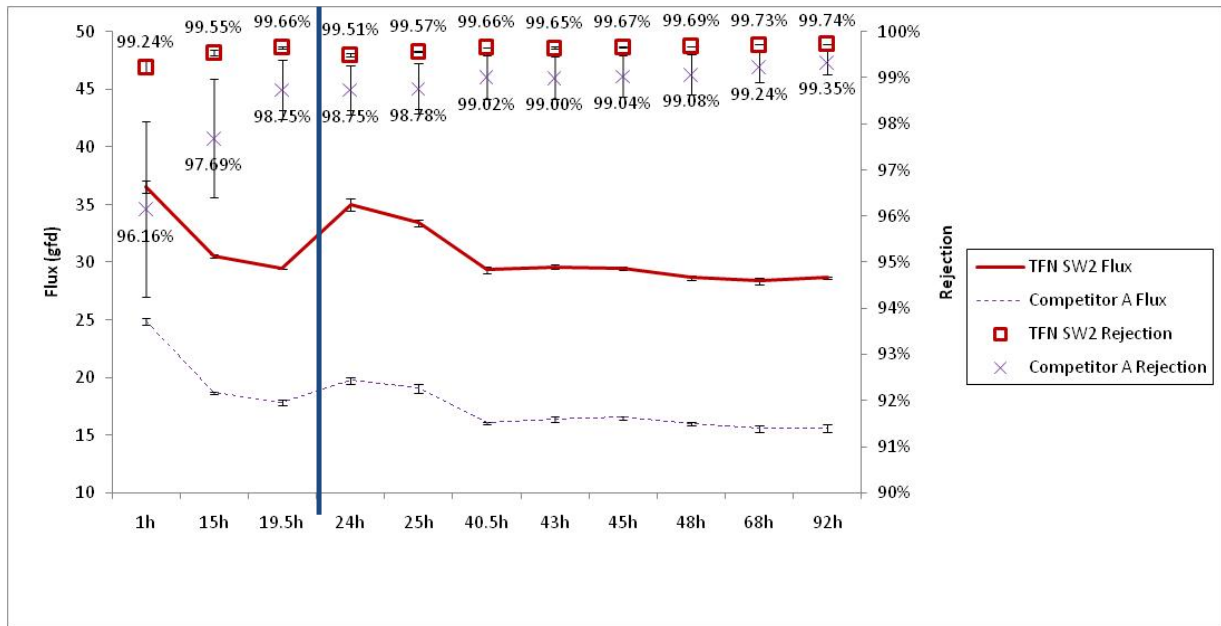


Figure 4: Membrane Performance vs. Competitor A. A cleaning was conducted at the location of the vertical bar at 20 hours.

Element Performance

Prior to fabrication of a coater optimized for TFN manufacturing, trials of several TFN formulations were made on an older 40” flat-sheet coating machine. Performance improvement versus a control formulation was evident in flat-sheet testing, although mechanical limitations of the machine prevented typical hand-cast performance from being obtained.

The membranes made were rolled into 4040 style elements and installed and tested at the SDTF. The fiberglass coated elements utilized a 5 leaf construction with approximately 70 sf of active area. A 30 mil propylene diamond feed spacer was used within the element.

One of the earlier elements made was left in place to evaluate the long-term performance. During the course of 10 months other elements were replaced, the position of the long-term element was altered, and various system operating conditions were investigated. Data in Figure 5 shows the normalized operating flux and rejection as a function of run time.

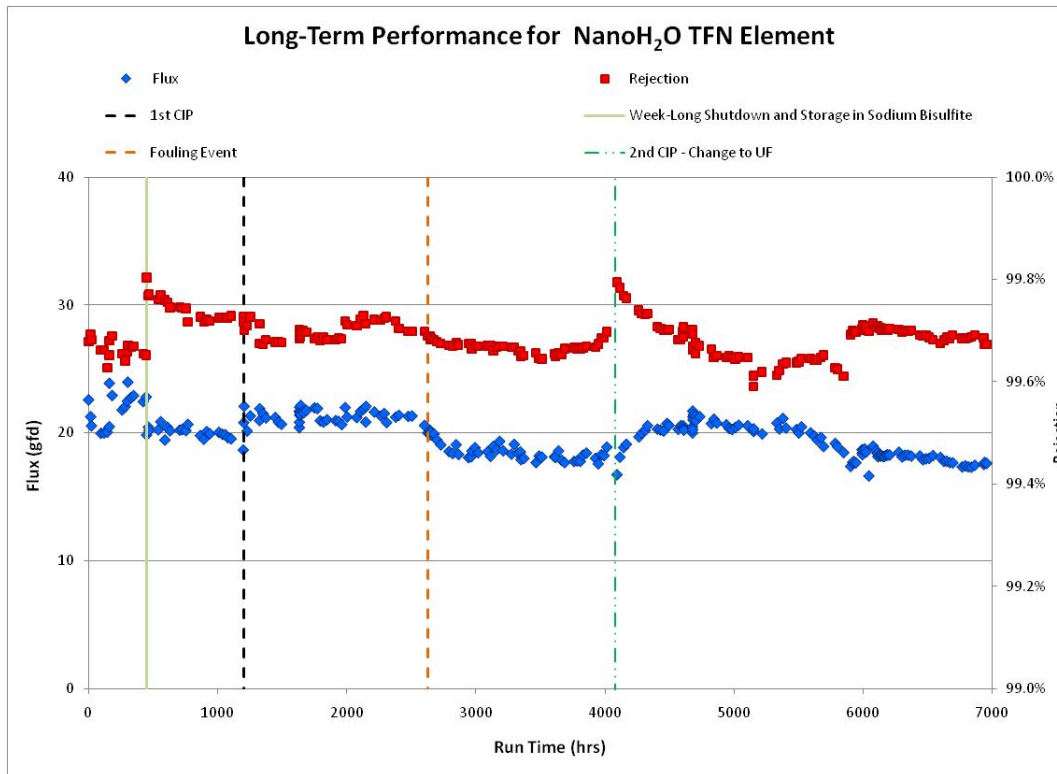


Figure 5: Long-Term Element Test

Fouling Event

After 4 months of operation (2,600 hrs) a red tide algal bloom in the waters around the SDTF intake resulted in a spike in SDI, particle count, and NTU of the incoming feed water at the facility for a period of 2 weeks (see Figure 6). At the start of this period the lead element was operating at a flux of 16.5 gfd and the element recovery was 5.3%. Over the course of the event the TFN module lost 14.3% of its permeability. When the membrane was next cleaned (two months later), the flux was recovered to within 95% of its pre-fouled state.

Although early lab studies had indicated some improvements in chemical structure and morphology that are thought to be related to fouling propensity (charge, roughness, hydrophilicity), the relatively modest performance loss, and subsequent flux recovery on cleaning through this red tide event was the first large-scale evidence that improved fouling properties may be present in some nanocomposite materials. Further testing will be needed to evaluate the repeatability and scope of any such improvement in properties.

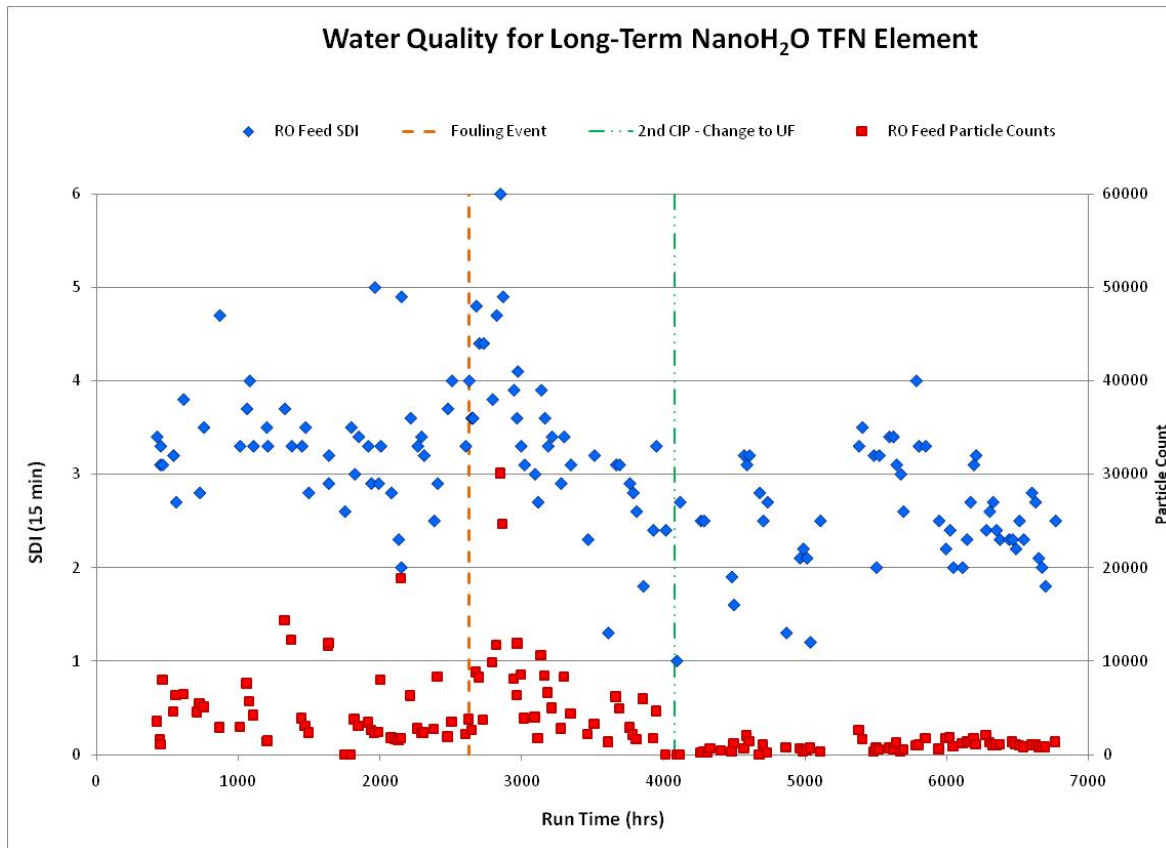


Figure 6: Particle count and SDI

Media vs. Membrane Pretreatment

After the fouling event and subsequent cleaning the intake water was switched from a media filter to a UF membrane pretreatment. An immediate improvement in treated water particle count was evident, and average SDI also improved from 3.4 on the media to 2.6 using the UF membrane. This behavior appeared quite stable over the period of time evaluated.

At this point, no clear conclusions can be drawn about the relative benefits of either pretreatment technology. Although one could argue that there appears to be a larger drop in flux with time using the membrane pretreatment, the media pretreatment didn't have a sufficiently long operational period to determine a fouling rate.

Clean-in-Place (CIP) Stability

An early question regarding TFN membrane applicability was its stability and performance through cleaning cycles. Certainly with the earliest published nanoparticles (Jeong et al, 2007) there was a potential that sufficiently high or low pH could chemically degrade the added nanoparticles, leaving holes in the separating layer and leading to an increase in salt passage.

As a means of determining chemical stability, a CIP was performed on the element early in its operation. After giving time for performance to stabilize (~1000 hrs), a CIP cycle was performed even though no loss in permeability had occurred. This CIP was used not to evaluate effectiveness of the cleaning agents with the membrane, but instead to evaluate the chemical stability of the separating layer. After the CIP, the measured flux and rejection matched initial performance. As nanoparticle degradation and/or deterioration of the nanocomposite matrix would have lead to a performance loss, this result indicates a stability of the TFN membrane to the conditions used.

A second CIP was performed later in the modules life after the fouling event previously described. After this cleaning, performance began to improve and eventually reached its baseline performance. Again, the stable flux and rejection suggest no evidence for chemical degradation.

Upcoming work will determine optimal cleaning conditions for TFN membranes after exposure to various fouling agents, as well as to determine compatibility and effectiveness of existing cleaning products.

Element Autopsy

Visual Inspection. Inspection of the element showed some particulates present on the feed. This is shown in Figures 7 and 8 below.



Figure 7: End caps. Feed on left, brine on right **Figure 8:** Close up of feed endcap

Once opened the membrane was observed to be slightly grey, with a brown wet deposit present (see Figure 9). After removal of the brown deposit, analyses were performed to identify the foulant.



Figure 5: View of membrane sheets

SEM/EDX analysis. The SEM overview (1000x) shown in Figure 10 reveals an organic deposit

with mineral elements embedded. On EDX profile, the main mineral elements detected are: S, Cl, Ca, Si, Al and Mg. Si and Al can originate from clays but also from algae. S can originate from the membrane itself (polysulfone support).

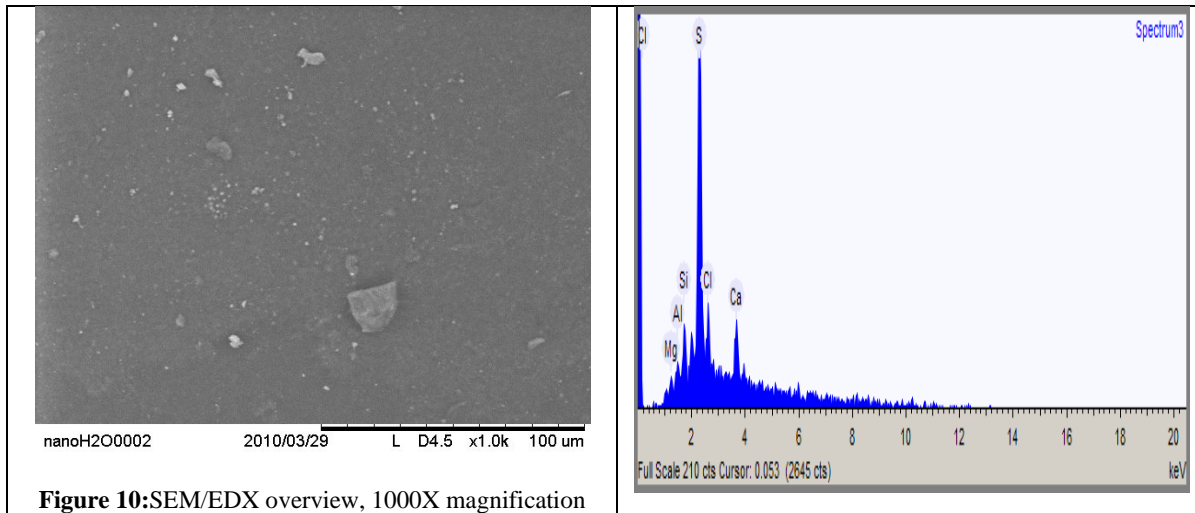


Figure 10:SEM/EDX overview, 1000X magnification

Foulant Analysis. Table 1 below shows the breakdown of the brown foulant layer. These data indicate the deposit presents mainly an organic fraction (85% of volatile matter), with a significant concentration of TOC (42.5 $\mu\text{g}/\text{cm}^2$) and total carbohydrates (10% of TOC). Biological results show a high number of total cells (3.21E+08), indicating a significant biological activity at the membrane surface.

Table 1: Chemical breakdown of the foulant removed from the membrane surface

	Amount present	
	(%)	($\mu\text{g}/\text{cm}^2$)
Dry matter	7%	91.3
Inorganic matter at 550C	15% (of dry)	13.8
Volatile matter at 550C	85% (of dry)	77.5
TOC		42.5
Total carbohydrates		9.4

ATR-FTIR Analysis. ATR-FTIR measurements were performed on the deposit. Results are displayed in Figure 12. The usual bands of a biofilm are observed: protein bands are observed at

1631 cm^{-1} and 1530 (amide I and amide II), polysaccharides band at 1022. The band at 1022 can also be linked to the presence of aluminosilicates (clays). Additional bands were also observed and are linked to specific compounds:

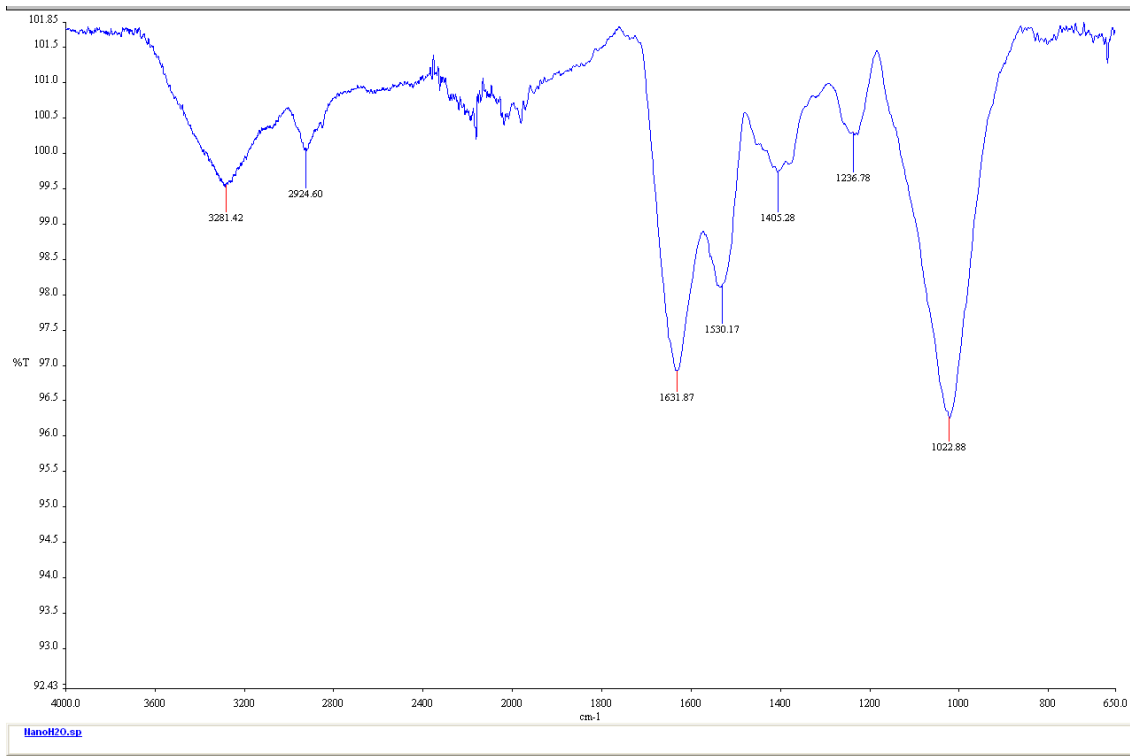


Figure 6: ATR-FTIR spectra of deposit

- An intense band around 3281 linked to O-H vibration (hydrogen bonded) or N-H vibration (secondary amides)
- A band around 2924 linked to C-H vibration (CH_2 and CH_3 groups), probably linked with the presence of humic substances

CONCLUSIONS

Optimized TFN membranes were compared with current commercial high flux SWRO products and found to have improved flux and rejection. These promising results from hand-cast membrane samples prompted efforts to scale-up to a continuous process enabling 40" wide membrane to be made, and elements to be manufactured. The resulting performance appears to validate the contention that with the appropriate procedures and techniques to prepare and handle the nanoparticle dispersions, a conventional coating machine and element fabrication facility can be used for scale up of the TFN membrane technology. Due to the relatively low mass of nanocomposite film used, only a minor effect on the total element cost is observed.

Operation of this TFN element technology over the course of this testing has given some insight as to the expected behaviour of this new membrane. The relatively stable flux and rejection has indicated the performance enhancement of the nanocomposite film is not a short-term performance enhancement, but rather a fundamentally different separation layer. Further, conditions that would

have lead to loss of nanoparticles would have also lead to an increase in passage; the lack of such a change supports the inherent stability of the nanocomposite film. This includes the high and low pH conditions used during the CIP cycles, as well as through mechanical stresses applied during repeated start-ups and shutdowns. Although further testing is needed to fully validate, the relatively modest flux loss and later flux recovery during a red tide event also suggests the possibility of improved tolerance to some biofouling events and may open up the possibility of increasing system design flux.

Autopsy of the element after testing was complete revealed the presence of materials consistent with operation in a biofouling-prone water including buildup of a largely organic mass containing microbiological materials. Effectiveness of prior cleaning cycles would indicate the relatively efficient removal of such materials from the membrane surface. Future testing side-by-side testing is recommended to better benchmark performance and cleanability in a field test site to commercially available products.

In the last 30 months, industrial research into nanocomposite RO membranes has resulted in the development of a new mixed matrix membrane material for seawater desalination. In this relatively short period, nanocomposite membranes have shown the potential for performance exceeding that of existing commercial products based on the standardized polymer chemistry used in RO membranes for the last several decades. This technology has now been further advanced and is in the process of being commercialized using a specially designed full-scale manufacturing line for a mid-2010 product release.

REFERENCES

USBR (U.S. Bureau of Reclamation and Sandia National Laboratories). (2003), *Desalination and Water Purification Technology Roadmap*: Springfield, Virginia.

Jeong B.H., Hoek E.M.V., Yan Y., Subramani A., Huang X., Hurwitz G., Ghosh A.K., Jawaor A. (2007), Interfacial polymerization of thin film nanocomposites: A new concept for reverse osmosis membranes. *Journal of Membrane Science*, **294** (1), 1-7.

Kurth CJ, Burk R., Green J. (2009), Leveraging nanotechnology for seawater reverse osmosis. In the IDA World Congress.

Ghosh A.K., Jeong B.H., Huan X., Hoek E.M.V. (2008), "Impacts of reaction and curing conditions on polyamide composite reverse osmosis membrane properties", *Journal of Membrane Science*, Volume **311** (1-2), 34-45.

Cadotte J.E. (1981), Interfacially synthesized reverse osmosis membranes. US4277344.

Dow (2010), System design: system performance projection. Technical manual excerpt, Form No. 609-02057-604.

Dubois M., Gilles K.A., Hamilton J.K., Rebers P.A., Smith F. (1956), Colorimetric method for determination of sugars and related substances, *Analytical Chemistry* **28**, 350–356.